Astron. Astrophys. 332, 235–244 (1998)

ASTRONOMY AND ASTROPHYSICS

Turbulence amplification in the atmosphere of pulsating stars: a first approach

D. Gillet[1], **J.F. Debiève**[2], **A.B. Fokin**[3], **and S. Mazauric**[4]

[1] Observatoire de Haute-Provence - CNRS, F-04870 Saint-Michel l'Observatoire, France (gillet@obs-hp.fr)
[2] IRPHE, UM CNRS Université d'Aix-Marseille I et II, 12 av. Général Leclerc, F-13003 Marseille, France
[3] Institute for Astronomy of the Russia Academy of Sciences, 48 Pjatnitskaja, 109017 Moscow, Russia
[4] von Karman Institute for Fluid Dynamics, 72 Chaussée de Waterloo, B-1640 Rhode-Saint-Genèse, Belgium

Received 21 July 1997 / Accepted 3 December 1997

Abstract. This paper is devoted to the understanding of the "missing temperature", called microturbulence by the astrophysicists, which appears when we want to modelize the width of stellar line profiles. In the framework of the two limiting turbulent regimes called "incompressible" and "pressure released", and expecting that the dissipation is negligible ("rapid distortion" or RDT case), it is shown that the turbulence amplification in the atmosphere of a radially pulsating star is not only due to the global compression of the atmosphere during the pulsation. Strong shock waves propagating from the deep atmosphere to the very low density layers also play a role in the turbulence variation, especially when they become very strong i.e., hypersonic. The predicted turbulence amplification induced by the global atmospheric compression is consistent with the solenodial RDT. For shocks, the predicted turbulence amplification in the "pressure released" regime is overestimated with respect to stellar observations when the compression rate becomes larger than 2 which corresponds to a limit Mach number near 2. Thus, when radiative effects take place, the present turbulence amplification theory breaks down. A new approach is required.

Key words: stars: individual: δ Cephei – Cepheids – line: profiles – turbulence – shock waves

1. Introduction

In all stars, the atmospheric gas is characterized by a "turbulent velocity" V_{turb}. This parameter has been introduced by astronomers to interpret the saturation portion of the curve of growth but there is no experimental or theoretical justification for its physical existence. What is the physical meaning of V_{turb}? In fact this velocity characterizes a *difference* between observed and theoretical atmospheric parameters affecting the full width at half maximum (FWHM) of an absorption spectral line. Because there are many other line broadening factors such as errors in oscillator strengths, magnetic fields, non-LTE effects, etc. which are not always taken into account in atmospheric models, there is no direct evidence that this "difference" would be only due to a turbulence. Nevertheless because a "sonic noise" induced by the subphostospheric convection is often present in the atmosphere, we expect that a turbulence field is present in stellar atmospheres. We estimate that V_{turb} only represents the upper limit of the true atmospheric turbulence which can be smaller than V_{turb} depending on the hydrodynamical phenomena occurring in the atmosphere.

Contrary to normal stars (i.e., stars with constant luminosity), the turbulent velocity of variable stars varies with the pulsation phase. For instance δ Cephei, a quite regular radially pulsating star (period of 5.4 days) discovered in 1784 by Goodricke, has one of the best determined turbulent velocities. Mel'nikov (1950) and later van Paradijs (1971) estimated its variation using the curve of growth method. It appears that V_{turb} presents a large peak around phase 0.8 i.e., at the minimum radius. The use of a set of static atmospheric models does not correctly take into account the large amplitude atmospheric fields and especially those induced by the propagation of strong shock waves. This can in part explain the smooth shape of the published V_{turb}-curves. As reviewed by Fokin, Gillet and Breitfellner (1996; hereafter FGB), a few theoretical works were devoted to the calculation of such curve. The most recent methods are based on a pulsating atmospheric model. They deduce V_{turb} from a comparison between theoretical and observational FWHM of a large set of metallic lines (Benz and Mayor 1982, Kovács and Buchler 1990) or with a single metallic line (Breitfellner and Gillet 1993, Stiff and Gillet 1994, FGB). In this last work, it emerges that velocity gradients play a major role in the broadening of metallic lines. This effect was already put into evidence in the atmosphere of non pulsating stars of spectral types O to late F in which high mass loss produces a velocity gradient in the photosphere (Kudritzki 1992, Lamers and Achmad 1994). Thus only FGB's work provides a realistic variation of V_{turb} vs. pulsation phase. Unfortunately, the time resolution of the obser-

vations was not large enough to give a well defined V_{turb}-curve. Only the large turbulent peak at phase 0.8 was determined with more precision.

Recently, Gillet et al. (1998) obtained 288 high resolution spectroscopic profiles of the unblended Fe I 5576.0883 Å absorption line of δ Cephei. Their observations cover three consecutive years. They determine a practically continuous FWHM curve vs. the pulsation phase. Using the FWHM as the relevant parameter, they compute a high time resolution turbulence curve. Their result shows that there are two different sources of turbulence variation. The first one is probably due to the global compression/expansion of the atmosphere during the pulsation. The second phenomenon is certainly the consequence of the passage of a few compressive and shock waves in the atmosphere. The first effect remains the main source of the turbulence variation, while shocks and the strongest compression waves provoke a few secondary turbulence peaks during the pulsational cycle. Their intensity seems connected to the wave amplitude.

What is the physical origin of the variation of V_{turb} in pulsating stars? For the sun, in spite of an appreciable convection field occurring in its atmosphere, $V_{turb} \simeq 2.3$ km/s remains constant with time (Takeda 1995). For pulsating stars, it seems natural to expect that the variation of V_{turb} would be mainly due to pulsations of the atmosphere. Indeed they induce large changes of volume (or density) between the minimum and maximum values of the stellar radius R. Breitfellner and Gillet (1993) obtained $\Delta R/R \simeq 0.13$ for some Fe I lines i.e., for a region located just above the photosphere. Moreover, because a few strong shock waves (see FGB) are generated during the pulsation cycle, they provoke local but large density increases in most atmospheric layers during their propagation. Thus, as already suggested by FGB, two turbulence amplification mechanisms can be expected. The first one would be the simple consequence of the global density variation of the atmosphere caused by the pulsation and the second would be due to strong local density increases induced by radiative shock waves. The aim of this paper is to quantitatively confirm these physical mechanisms.

In Sect. 2 we briefly present the non-linear non-adiabatic model used to describe the pulsation of the atmosphere of the variable star δ Cephei. Turbulence models are discussed in Sect. 3. Results are analysed in Sect. 4 and the special case of very strong shocks is examined in Sect. 5. Finally some comments and concluding remarks are given in Sect. 6.

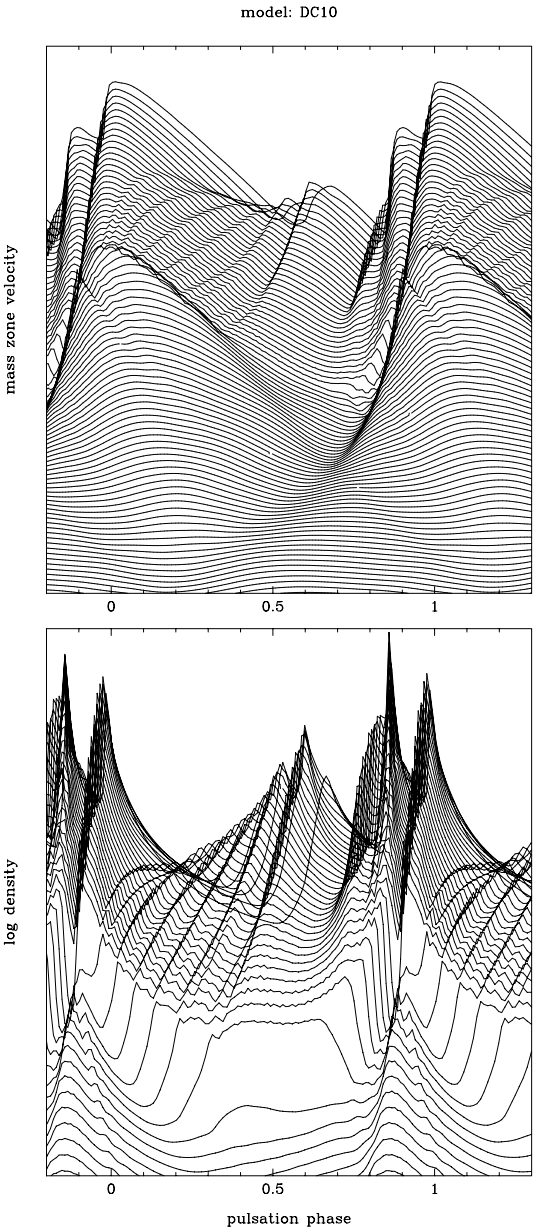

Fig. 1. Theoretical velocity (top) and density (bottom) variations with phase for different mass zones traced over 1.5 pulsation cycles of the classical Cepheid model δ Cephei. The maximum and minimum radii occur about at phases 0.37 and 0.85 respectively (see FGB). Note that an arbitrary shift has been done between each mass zone to help the visibility. This explains the absence of velocity and density scales

2. Non-linear non-adiabatic pulsational model

2.1. Three main shock waves

A non-linear non-adiabatic pulsational model (model A or DC10) of the classical Cepheid star δ Cephei has already been discussed by FGB. It is characterized by an extended atmosphere, and the parameters of this model are $T_{\rm eff} = 6056$ K, $L = 3100\,L_\odot$, $M = 7.0\,M_\odot$, $X = 0.7$ and $Y = 0.28$. The total mass zone number is 100, the outmost mass zone is labeled 100. Fig. 1 shows the theoretical velocity and density variations vs. the pulsational phase for different mass zones. The most striking feature is the appearance of a few waves and shock waves per cycle. Three main shocks, s1 (phase 0.72 at the mass zone 80), s2 (0.92) and s3 (0.50) and a series of faint waves that we call "buzz waves" occur just above the photosphere in the phase interval 0–0.4, are well visible (see also Fig. 3 of FGB). The exact phase of the appearance of a shock is model dependent.Thus sometimes an appreciable phase shift (near 10%) can be noticed between the observations and the model. The main shocks provoke appreciable local compressions because they are radiative

which at the limit of an isothermal shock gives a compression ratio $\eta = M^2$, where M is the upstream Mach number. In the case of our model of δ Cephei, eta reaches 28 in the shock s1 at the layer 96, while it is small (η = 3.5) at the layer 80 and very small (η = 1.5) at the photospheric level (around layer 74). The compression ratio η for s2 is 6.3, 8 and 13 for layers 74, 80 and 96 respectively and it remains always small (1.6, 2.7 and 4.0 respectively) for s3. This shows that the shock intensity is strongly dependent on the shock altitude. Thus hypersonic shocks ($M > 5$) i.e., shocks which can excite degrees of freedom of atoms and molecules, only exist in the highest part of the atmosphere in our δ Cephei model.

2.2. Fe I line formation region

The Fe I line at 5576.0883 Å is formed in an atmospheric region located between the photosphere (line wings) and a mass zone between 84 and 95 (line core) depending of the pulsation phase (see Fig. 3 of FGB). This region represents about 98% of the mass of the atmosphere ($3\,10^{-6}\,M_*$) but only 20% of its average radial extension which varies between 2 and 6 % of the stellar radius ($64\,R_\odot$). The contribution of each mass zone of the line formation region to the emerging line intensity is not constant. The flux contribution versus the formation depth and the line profile wavelength is given by the so-called *contribution function* (CF). Up to now, the CF assumed a static atmosphere (see for instance Achmad, de Jager and Nieuwenhuijzen, 1991). Nevertheless, Albrow and Cottrell (1996) have recently shown that the pulsational velocity field has an appreciable effect on the results deduced from static CF and that the calculation of the relevant CF was extremely CPU time consuming. Consequently, hereafter in the framework of our semi-quantitative approach, the FWHM part of the line is simply assumed to be formed around the mass zone number 80, corresponding to about the middle of the line forming region (LFR). We have checked that the results deduced in this paper are weakly sensitive to a plausible choice of this mass zone number.

3. Available turbulence models

We have first restricted our present study to limiting cases where the dissipation is negligible or do not have sufficient time to act on the amplification mechanism. This approach is called "rapid distortion theory" or RDT. Moreover, observations show that two cases $M_t \ll 1$ and $M_t \simeq 1$ can occur during the pulsation. $M_t \equiv u^{'}/c_s$ is the turbulent Mach number, $u^{'}$ is the scale of velocity fluctuation and c_s the sound velocity. $M_t \ll 1$ corresponds to the case where the divergence of the fluctuating part of the velocity is negligible ($u^{'}_{ii} \simeq 0$) i.e., we are in the so-called "incompressible turbulent regime". The second turbulent regime ($u^{'}_{ii} \neq 0$) takes place when compressible effects become appreciable and especially, when the compression is strong, a very simple limiting case occurs; it is called the "pressure released regime". Indeed, in the intermediate cases the solution is quite complex because the initial spectrum must be specified precisely and if necessary a correct modelling of the dissipation must be proposed.

3.1. Incompressible turbulent regime ($M_t \ll 1$)

3.1.1. k-ϵ model

Firstly, we examine the "coarse" two-equation model called k-ϵ for two reasons. One is to obtain an estimation for the kinetic energy amplification in order to degrade the model to the case of a rapid distortion. Secondly, the Coleman and Mansour (1991) version has indicated some dependency of the dissipation on the temperature for an adiabatic spherical compression. Using the same idea, has the dissipation a reasonable behaviour in a non-adiabatic process such as the pulsation of the atmosphere of a Cepheid star? The following formulation is an adaptation of the Coleman and Mansour version to the case of a non-adiabatic mean flow. This allows us to evaluate the amplification of a compressible homogeneous turbulence submitted to a spherical compression, with only time dependent mean pressure and temperature.

The turbulent kinetic energy k is defined by

$$k \equiv \frac{1}{2}\frac{\overline{\rho\, u_i^{'} u_i^{'}}}{\overline{\rho}} \tag{1}$$

where $u_i^{'}$ corresponds to the velocity fluctuations in a density weighted average (Favre average). The equations of the turbulent kinetic energy k and the evolution of the dissipation energy ϵ write (see Appendix A)

$$\frac{dk}{dt} = -\frac{2}{3}Dk - \epsilon \tag{2}$$

$$\frac{d\epsilon}{dt} = -\left[\frac{1}{3}D + n\Theta\right]\epsilon - C_2\frac{\epsilon^2}{k}. \tag{3}$$

where n is a constant characterizing the interaction force between particles of the gas ($n = 1/2$ for a perfect gas), C_2 = 1.92, $D \equiv -dln\overline{\rho}/dt$ and $\Theta \equiv -dln\overline{T}/dt$. This system of equations constitues the k-ϵ model.

If during compression the dissipation is negligible compared with turbulent energy production, the following constraint called the *condition of rapid distortion* is satisfied

$$\left|\frac{Dk}{\epsilon}\right| \gg 1. \tag{4}$$

This parameter is of the order of the initial ratio between the average life time τ_{turb} of an eddy (cascade time) and the time D^{-1} characterizing the rapidity of the variation of the mean field

$$\left|\frac{Dk}{\epsilon}\right| \sim \frac{\tau_{turb}}{D^{-1}}. \tag{5}$$

By definition the condition Eq. (4) is satisfied in RDT. In the limiting case where $|Dk/\epsilon|$ is infinite, the second term of the

right side of Eq. (2) and the third term of Eq. (3) are zero, and the equations are not coupled anymore

$$\frac{dk}{dt} = -\frac{2}{3}Dk \tag{6}$$

$$\frac{d\epsilon}{dt} = -\left[\frac{1}{3}D + n\Theta\right]\epsilon. \tag{7}$$

So the k-ϵ system can be analytically solved

$$k(t) = k(t_0)\exp\left(-\frac{2}{3}\int_{t_0}^{t} D(t')dt'\right) \tag{8}$$

$$\epsilon(t) = \epsilon(t_0)\exp\left(-\frac{1}{3}\int_{t_0}^{t} D(t')dt' - n\int_{t_0}^{t}\Theta(t')dt'\right). \tag{9}$$

Because $D(t) = -\frac{d\ln(\rho(t))}{dt}$ and $\Theta(t) = -\frac{d\ln(T(t))}{dt}$, we obtain

$$k(t) = k(t_0)\eta^{2/3} \tag{10}$$

$$\epsilon(t) = \epsilon(t_0)\eta^{1/3}\theta^n \tag{11}$$

where $\eta \equiv \overline{\rho}(t)/\overline{\rho}(t_0)$ is the density ratio and $\theta \equiv \overline{T}(t)/\overline{T}(t_0)$ the temperature ratio. Note that in a non-adiabatic compression (this case), the dissipation is smaller than that in an adiabatic case because $T < T_{adia}$. Thus, from Eqs. (10) and (11), it appears that the dissipation is not strongly affected either in adiabatic or non-adiabatic cases if the dependence of dissipation on the temperature only occurs through the molecular viscosity (see Appendix A). If we suppose that the mean movement is a periodic pulsation (compression and expansion), then the density ρ, the turbulent energy k and its dissipation rate ϵ are periodic functions. Eqs. (10) and (11) are only valid during the time interval of the order D^{-1} characterizing the variation of the mean flow. In fact, we will apply these equations over a pulsation period which is of the order of magnitude of D^{-1}.

3.1.2. Solenoidal RDT

Because for Cepheid stars, the curvature is very small, we assume that the atmospheric distortion is not *locally* spherical but practically axial. Thus compression must induce a preferential amplification direction i.e., we cannot assume that the turbulence remains isotropic during the compression. In the anisotropic case, in order to evaluate the importance of the amplification in the framework of a rapid distortion, we use the model of Jacquin, Cambon and Blin (1993, hereafter JCB) which considers an adiabatic homogeneous axial compression. They show that the amplification of the turbulent kinetic energy is limited by two analytical solutions. The first one called "solenoidal" is obtained when $M_t \ll 1$. Note that because the RDT applies and

$$\left|\frac{Dl}{c_s}\right| \simeq \left|\frac{Dk}{\epsilon}\right| M_t \tag{12}$$

where l/c_s is the time of propagation of a compression in an eddy of size l. We have also the condition of incompressibility $|Dl/c_s| \ll 1$ as used by JCB. For an initial isotropic turbulence these authors find again the relation

$$k(t) = \frac{k(t_0)}{2}\left(1 + \eta^2\frac{\tan^{-1}\sqrt{\eta^2-1}}{\sqrt{\eta^2-1}}\right), \tag{13}$$

already obtained by Ribner and Tucker (1953). This relation gives the *minimum* amplification associated with an axial compression.

3.2. "Pressure released" regime

The second limiting solution (called by JCB "pressure released") represents the *upper limit* of the amplification process. It occurs when the parameter $M_t > 1$, which can also be written in the case of rapid distortion $|Dl/c_s| \gg 1$. This case takes place when the compressibility becomes important i.e., when one neglects any influence of the fluctuating part of the pressure. The result is

$$k(t) = \frac{2+\eta^2}{3}k(t_0). \tag{14}$$

This expression was obtained by JCB in the case of a rapid axial compression, but to allow an analytical treatment they suppose an homogeneous turbulence and an isotropic initial turbulence. But for a normal shock (inhomogeneous medium) this expression was also directly obtained by Debiève, Gouin and Gaviglio (1982) and Debiève (1983), who consider the discontinuity of the Reynolds stress tensor $R_{i,j} \equiv \overline{u_i' u_j'}$ with an hypothesis of zero pressure fluctuation. Thus, whereas the RDT predicts a continuous increase of k proportional to the density ratio η in the incompressible turbulent regime, we have a faster amplification (proportional to η^2) in the "pressure released" regime.

The amplification factor $k(t)/k(t_0)$ of the turbulent energy given by Eqs. (10), (13) and (14) only depends on the initial and final average densities of the gas ($\eta \equiv \overline{\rho}(t)/\overline{\rho}(t_0)$) and not on the evolution of ρ between the initial and final times. Thus these amplification factors are not influenced by the shape of $D(t)$.

4. Turbulence amplification

High resolution spectroscopic observations of δ Cephei – more precisely, measures of the FWHM of the Fe I line $\lambda\lambda$5576.0883 – have recently permitted Gillet et al. (1998) to determine a high time resolution turbulence curve. They show that the turbulent energy ratio $k_{\max}/k_{\min}$ at maximum increases by a factor of around 10–15 that at the minimum stellar radius i.e., during the maximum atmospheric compression. In addition these authors show that compression waves and shock waves also produce a turbulence increase (see their Fig. 2b) but of smaller amplitude. Thus two amplification mechanisms must be considered to explain the observations. The first one would be as a consequence of the global atmospheric compression and is discussed in Sect. 4.1, while the second must be due to the passage of a (shock) wave in the atmosphere where the spectral absorption line is formed (see Sect. 4.2).

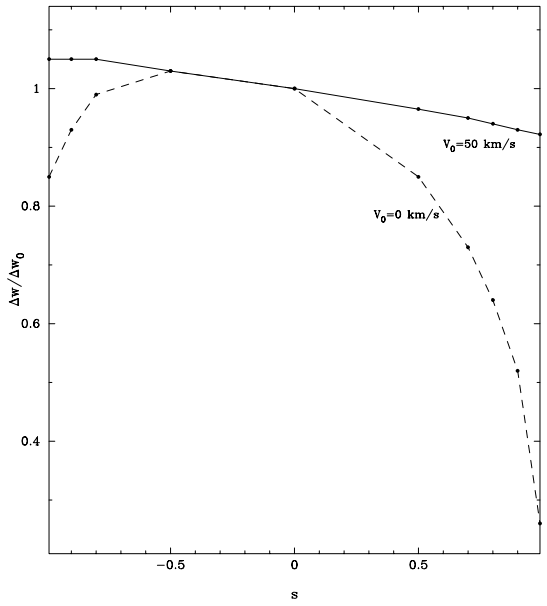

Fig. 2. Effect of an anisotropic turbulence on the broadening of a metallic line (Fe I 5576.0883 Å). s is the anisotropy coefficient which is equal to -1, 0 and +1 respectively when the turbulence is tangential, isotropic or radial. V_0 is the pulsational velocity and ($\Delta\, w/\Delta\, w_0$ the ratio between the FWHM of the line when the turbulence is anisotropic and isotropic respectively

We have no direct information about the mean size l of turbulent eddies and, consequently, on the spectral distribution of turbulent kinetic energy among the various eddies. Nevertheless, if the RDT criterion is assumed valid then we can estimate the typical limit size of the relevant eddies. Indeed, because $k \simeq u^{'2}$ and $\epsilon \simeq u^{'3}/l$, the RDT criterion Eq. (4) becomes

$$\left|\frac{Dk}{\epsilon}\right| \sim \left|\frac{Dl}{u^{'}}\right| \tag{15}$$

where D is given by the mean flow conditions deduced from the pulsating model and the turbulent velocity $u^{'}$ is estimated from the observations (between 2 and 8 km/s for δ Cephei, Gillet et al. 1998). Thus, depending on the l-value determined with respect to the atmospheric thickness for example, we can test the applicability of the RDT. It is also interesting to recall that, for $|Dk/\epsilon| \gg 1$, the turbulence amplification already reaches its maximum possible value while smaller values of $|Dk/\epsilon|$ necessarily give a weaker amplification.

An interesting point is the effect of an anisotropic turbulence over the measured turbulence i.e., over the observed line profile. Since we have a preferential direction of the gas deformation (the shock direction), the turbulence can be anisotropic, i.e. the radial component of the turbulent energy can differ from the tangential components. In this case, the difficulty is that the observed turbulence (in the line of sight) is a combination of radial and tangential components of the Reynolds stress tensor integrated over the half stellar sphere. Only in the case of isotropy, the measured turbulence in the line of sight is proportional to the turbulent kinetic energy. To evaluate the relation between the measured turbulence and the turbulent kinetic energy, we assume that each surface element is characterized by the so-called *intrinsic* intensity line profile which, if the Stark broadening contribution is negligible, is assumed to be Gaussian (see Appendix B). Fig. 2 shows the line broadening effect on a metallic line vs. the anisotropy coefficient s with or without a mean dilatational (i.e. radial) stellar velocity V_0. $\Delta\, w/\Delta\, w_0$ is the ratio between the FWHM of a metallic absorption line when the turbulence is anisotropic and isotropic respectively. s is the anisotropy coefficient (see Appendix B) which is equal to $-1, 0$ and +1 respectively when the turbulence is tangential, isotropic and radial. With conditions defined in Appendix B, the departure from isotropy is less than 15 % when $-0.9 < s < 0.5$ for V_0 = 0 km/s, while it remains smaller than 10 % when a mean dilatational field is present (V_0 = 50 km/s). On the other hand, the anisotropic effect is stronger when the turbulence is radially polarised ($s > 0.5$). Thus it appears that this anisotropic effect noticeably decreases with V_0 i.e., it becomes weaker and weaker when the shock Mach number increases. Consequently, we have not considered this effect hereafter.

4.1. Pulsation without shock waves

We first study the turbulence amplification during a compression in the unperturbed atmosphere of δ Cephei without the presence of waves. For this we choose the density evolution of the zone number 80. However, we have to modify this evolution in order to eliminate all perturbations due to shocks. We simply deduce it from the real average density profile given by the pulsating atmospheric model (Sect. 2). Fig. 3 shows both these real and synthetic density curves. By chance no shocks are crossing the layer 80 during the phase of minimum radius ($0.8 < \phi < 0.9$).

The value of D rapidly varies between $-2.5\,10^{-4}\,\mathrm{s}^{-1}$ up to $8\,10^{-5}\,\mathrm{s}^{-1}$ around the minimum radius ($0.7 \leq \phi \leq 0.95$) while outside this phase range the D-value remains very small ($\leq 10^{-5}\,\mathrm{s}^{-1}$). Consequently, because $u^{'}$ is between 2 and 8 km/s (Gillet et al. 1998), the condition of rapid distortion (Eq. (4)) needs to have eddies of size $l \gg \Delta\, R_{atm}/50$ (at R_{min}) and $\Delta\, R_{\mathrm{atm}}/2$ (at R_{Max}), where $\Delta\, R_{\mathrm{atm}}$ is the atmospheric thickness. Eddies of this dimension are problably at the upper limit of reality. On the other hand, the condition of incompressibility $|Dl/c_s| \ll 1$ is valid when $l \ll \Delta\, R_{\mathrm{atm}}/50$ (at R_{min}) and $\Delta\, R_{\mathrm{atm}}$ (at R_{Max}) because the sound velocity is between 6 and 7 km/s depending on the pulsation phase. Finally, we consider that the use of the amplification formula (Eqs. (10) and (13)) are at the limit of their applicability.

Fig. 4 shows the amplification factors for the k-ϵ and the solenoidal RDT models compared to observations. The k-ϵ approach predicts an amplification 2 times smaller than the observations at the amplification maximum, while there is only a difference of 10 % with the solenoidal one. This shows that the anisotropic amplification induced by the radial expansion of the atmosphere must be taken into account. This adequate result was not in principle expected because as assumed before, the incompressibility condition $|Dl/c_s| \ll 1$ breaks down when the turbulent Mach number is close to unity as exists around the

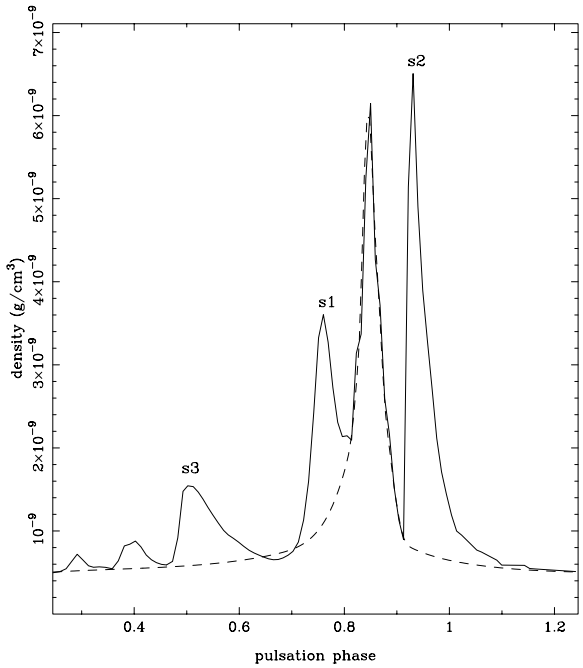

Fig. 3. Density of the layer 80 vs. phase. The tree main shock waves s1, s2 and s3, respectively at phases 0.72, 0.92 and 0.50, provoke strong and rapid increase of density when they come into the layer, which rapidly decreases when they leave (see FGB). The dashed line represents the expected density variation without shocks. The maximum at phase 0.85 corresponds to the minimum radius

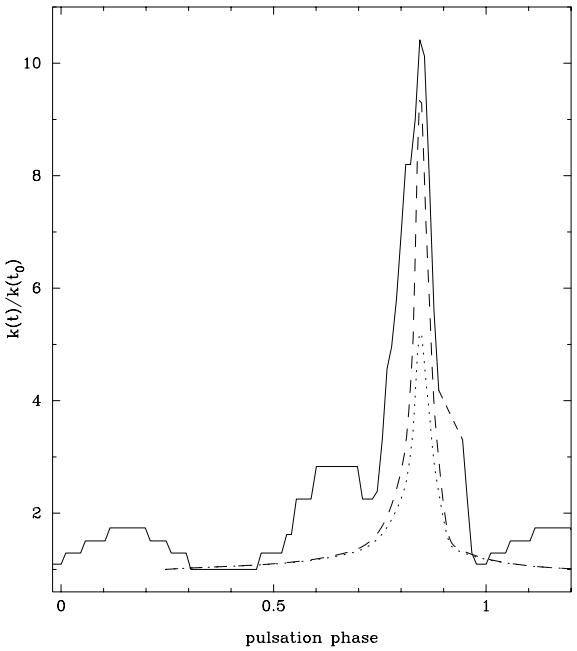

Fig. 4. Observed and predicted amplification factors $k(t)/k(t_0)$ vs. pulsation phase. Theoretical curves are obtained for the case when no shocks are present in the atmosphere. The continuous line shows the result obtained by Gillet et al. (1998) based on the observation of the FWHM of the Fe I line at $\lambda\lambda$5576.0883 and a non-linear non-adiabatic pulsating model. The dotted line corresponds to the k-ϵ model (Eq. (10)) and the dashed line to the solenoidal RDT (Eq. (13)). Note the breakdown around the phase 0.9 in the continuous turbulence curve due to a numerical limitation of the pulsating model

minimum radius (phase 0.85). Moreover, following the same applicability conditions, these two approaches are well adapted around the maximum radius (phase 0.37) where u' is minimum (2 km/s). We can see from Fig. 4 that they give the same amplification in the phase interval 0.0–0.6 (difference smaller than 1 %). Thus the amplification remains isotropic up to an amplification of about 17 %.

The FWHM of the observed peak appears larger in the phase interval 0.76–0.83 while it is similar during the fast turbulence decrease near phase 0.88. This is probably due to the presence of the shock wave s3 which crossed the Fe I line formation region during the phase interval 0.76–0.83.

4.2. Pulsation with shock waves

According to the result of Sect. 4.1, we have to take into account the propagating shock waves in the atmosphere and see how the turbulent velocity is amplified during local shock compression. When a stellar shock wave is not strong i.e., when the upstream Mach number is smaller than approximately 5, we can expect that the electronic degrees of freedom of atoms are not excited. In this case the shock essentially remains *adiabatic* and the density jump η is limited by the classical relation $\eta \leq (\gamma{+}1)/(\gamma{-}1)$. For instance, in a diatomic gas with rotational degrees of freedom completely excited, $\eta = 6$, and if in addition all vibrational levels are excited, then $\eta = 8$. When electronic levels begin to be populated, then, in addition to the adiabatic shock front, a radiative shock wake appears in which the excitation and subsequent relaxation of internal degrees of freedom of particles take place. The wake thickness is considerably larger than that of the front. When the Rankine-Hugoniot relations are applied over a region including both the shock front and the radiative wake (i.e., the shock wake structure is not explicitly calculated), the density jump strongly increases due to dissociation, ionization and recombination effects. In this case the above jump relation is no longer valid and only the Rankine-Hugoniot relations including the radiative terms provide the true density jump. For large Mach numbers (between 10 and 40 depending on the type of gas), the shock becomes isothermal and the density jump is $\eta \simeq M^2$. An estimate of the thickness of a radiative shock wake is given by the cooling time τ_c i.e., the time necessary for the shocked material to return to radiative equilibrium. Given the densities and temperatures in the atmosphere of δ Cephei, τ_c is of the order of 1 s. This time corresponds to the upper limit of the compression time D_s^{-1} induced by the shock. It is overestimated in our pulsating atmospheric model because the numerical method uses an artificial viscosity. Nevertheless, the predicted value of the density jump far from the shock front is realistic because it results from the conservation equations. Finally, for all types of shocks (from adiabatic to isothermal), $D_s^{-1} < 1$ s. Note that from Fig. 3 (layer 80), the density jumps in shocks s3, s1 and s2 are 2.7, 3.5 and 8.0 respectively. The upstream Mach number for s3 is around 2 and for s1, $M > 6$.

Thus, s3 is certainly adiabatic, s1 almost adiabatic and s2 certainly non-adiabatic.

With physical conditions occurring in the atmosphere of δ Cephei when shocks are present, the compressibility criterion $|D_s l/c_s| \gg 1$ is satisfied if $l > 1$ km. This typical eddy size l is very small compared to the atmospheric thickness, which is between $7\,10^5$ km and $2\,10^6$ km depending of the pulsation phase. Consequently we can expect that we are always in the "pressure released" regime in the presence of shocks. On the other hand, because the turbulent Mach number $M_t \equiv u'/c_s$ is $0.1 < M_t < 1$, Eq. (12) shows that we are in the RDT regime ($|Dk/\epsilon| \gg 1$). Thus we can consider that the dissipation is negligible and we can apply the amplification relation Eq. (14).

From Eq. (14), we must expect an amplification of the turbulent kinetic energy k/k_0 around 3, 13 and 22 for s3, s1 and s2 respectively. s2 crosses the Fe I formation region at a phase of approximatively 0.92. Unfortunately Gillet et al. (1998) could not predict for this shock any turbulence amplification (Fig. 4) due to a numerical artefact occurring between phases 0.89 and 0.94. Moreover, their spectroscopic observations giving the FWHM-curve of the Fe I line (see their Fig. 1) do not show any FWHM bump near phase 0.92. Consequently, because the expected amplification is very large (k/k_0 = 22) and the time resolution of the observations is very good, we can conclude that an appreciable and short turbulence increase certainly does not exist at this phase. For s1 a phase shift appears. Indeed, the model gives a phase of 0.72 while observations suggest that it occurs near phase 0.77 (Fig. 4). We interpret the noticeable asymmetry on the short phase side of the large peak centered at phase 0.83 as the consequence of the shock s1. Although the predicted turbulence amplification (k/k_0 = 13) is substantial, a local bump is not observed within the FWHM curve. Gillet et al. (1998), taking into account several significant line broadening processes taking place during this part of the pulsation cycle, show that s1 induces a smaller amplification, near 2. This is several times weaker than the expected value from Eq. (14). The weakest shock s3, which is also phase shifted from 0.50 to 0.65, gives an amplification near 2.5 (Gillet et al. 1998). This is consistent with the value of 3.0 predicted by Eq. (14).

Finally, it appears that the turbulence amplification provoked by a shock wave passage is well predicted by the pressure released regime given in Eq. (14) only when the shock intensity remains weak i.e., when the shock is not radiative. This equation was obtained in the framework of the adiabatic hypothesis. Consequently, it is not surprising that the calculated amplification rate is overestimated in gases in which the radiative energy becomes more and more predominant. Indeed, in such a situation, the radiative flux term is no longer negligible in the energy equation and we can expect from the above results that it plays a major role. This occurs when a large part of the gas energy is stored in the internal degrees of freedom of particles, contrary to all available turbulence models in which gas particles are considered like hard spheres.

A result is that, in this case, a modified theory of the turbulence amplification is required to explain the weak amplifications observed when the shock compression is larger than 3.

5. Limiting case of very strong shocks

RR Lyrae stars are a famous group of radially pulsating stars characterized by very strong shock waves, contrary to classical Cepheid stars such as δ Cephei in which shock intensities remain moderate. For instance Fokin and Gillet (1997) showed that there were shocks with a final velocity amplitude between 120 and 170 km/s. With a sound velocity in the highest atmospheric layers around 7 km/s, the upstream Mach numbers are between 17 and 24. Thus for this class of variable stars we have a hypersonic gas, so the shocks are almost isothermal. Consequently, we must expect that the turbulence amplification would be very large because, for isothermal shocks, the compression ratio is $\eta \simeq M^2$. Note that other groups of pulsating stars such as BL Herculis, W Virginis and RV Tauri stars also exhibit hypersonic shocks.

As discussed at the beginning of the previous section, a shock wake is a hot and compressed region. It is much larger than the (adiabatic) shock front. All numerous eddies of fluid particles and vortices which characterize the observational turbulence traverse the shock wake. When the shock intensity is weak, the downstream physical conditions remain moderate and consequently the gas is weakly radiative. In these conditions, the temperature and pressure in the wake are not large enough to strongly dissociate and ionize atoms and molecules. This is not the case when the shock intensity increases because the gas is more and more heated and compressed. The unperturbed turbulent gas is characterized by an initial turbulent spectrum depending on upstream physical conditions. Thus, at the limit of the strongest shock waves, we expect that the eddy distribution after recombination processes in the wake would be only determined by the thermodynamic and hydrodynamic conditions in this region. Finally this means that the turbulent spectrum just after the radiative shock wake would not be influenced by the upstream turbulent spectrum.

6. Conclusion

In this work we have assumed that the mean flow variables are not strongly affected by the turbulent state of the gas because we have always used the same "mean" atmospheric model. This is certainly justified as long as the amplitude of the fluctuating part remains moderate with respect to the mean value i.e., as long as we are far from "supersonic" turbulence.

In the case of a typical pulsating star (δ Cephei), we have shown that we can explain the turbulence amplification due to the global atmospheric compression. The solenoidal RDT appears to give a better quantitative prediction than the k-ϵ model. Always in the framework of the rapid distortion approach and in the limiting case of the "pressure released" regime, only turbulence amplifications by shocks inducing a maximum compression rate around 3 are acceptable. For stronger shocks, we obtain a considerable overestimation of the amplification. In other words, the available amplification theories of turbulence are valid for weak shocks i.e., for Mach numbers approximately smaller than 2. What is the physical reason of this amplifica-

tion limitation? Basically, the main obvious difference between weak and strong shocks is the occurrence of the excitation of degrees of freedoom of particles. Indeed, for stellar atmospheric gases, the excitation of atoms and molecules take place for Mach numbers near 2. Consequently, it seems natural to expect that the effects induced by radiative terms into conservation equations are at the origin of the observed limitation of the turbulence amplification. The best direction for future investigations is certainly there.

The linear model used to describe the turbulence takes into account the presence of shock waves only through rapid variations of the density. Nevertheless, it seems necessary to understand the complex interactions between the gas and the shock discontinuity. In addition to the above main effect (mean flow compression), two secondary effects – the vorticity generation due to shock front curvature and turbulent kinetic energy generation caused by the unsteady movement of the shock front – must be considered through the so-called linear interaction analysis or LIA (Lee, Moin and Lele 1992). Ribner (1954) has first proposed such a description of the turbulence amplification but it was limited to a weak shock wave. It is based on the *adiabatic* Rankine-Hugoniot relationships. In the atmospheres of pulsating stars, the propagating waves are strong shocks (upstream Mach number larger than 5), thus they are interacting with translational, electronic, vibrational and rotational states of molecules of the gas. Consequently, an extension of the Ribner theory to the non-adiabatic case must certainly be useful to explain the turbulence amplification in pulsating stars.

Jacquin, Cambon and Blin (1993) have investigated the amplification of turbulence in an axial compression in the framework of the homogeneous rapid distortion theory (RDT). Their linear and adiabatic approach only accounts for the mean compression of the shock and consequently other secondary interactions are ignored. Moreover, because the compression of the turbulence field by a shock wave is rapid and inhomogeneous contrary to RDT assumptions, we must expect that RDT is certainly inappropriate to predict *quantitative* amplification rates. Similar work was been done by Lee, Moin and Lele (1992). It appears that RDT gives a very large turbulence amplification at high Mach numbers (12 at an upstream Mach number of 10), contrary to Ribner's LIA (limited to an amplification factor of 2 by the use of the density jump Rankine-Hugoniot relation). Direct numerical simulations such as Rotman (1991), Hannappel and Friedrich (1995) or Mahesh et al. (1997) (see Friedrich and Bertolotti 1997 for a recent review) also show small amplifications because they assume that particles have no internal degrees of freedoom i.e., the gas is adiabatic. This is consistent with the LIA result because it uses the adiabatic Rankine-Hugoniot jump conditions and assumes the adiabatic gas. Finally all these results show that the problem of the interaction of isotropic turbulence with a strong shock wave cannot be understood in the framework of these approaches.

An interesting test will be given by the limiting case of very strong shocks. Indeed, it appears that the quantitative estimate of the amplification of the turbulence does not depend on the upstream turbulence state. Observational comparisons with some astrophysical stellar objects in which very strong shocks occur will be helpful.

Acknowledgements. The work of ABF has been done in part under the auspices of the Ministère de l'Enseignement Supérieur et de la Recherche (grant 149179B) during a six-months stay at the Observatoire de Haute-Provence. ABF also acknowledges the support of the Russian Foundation for Fundamental Researches (grant 95-02-06359). The authors are grateful to Dr. P. Cottrell for his useful suggestions to improve the clarity of the paper.

Appendix A: k-ϵ model

The turbulent kinetic energy rate is given by the trace of the product of the fluctuation of the Navier-Stokes equations by the velocity fluctuations i.e., the trace of the Reynolds equations (see for instance Mohammadi and Pironneau 1994)

$$\frac{dk}{dt} = -\frac{1}{\overline{\rho}}F_{j,j} + W + \Delta + P - \epsilon \tag{B1}$$

where $F_{j,j}$ is shorthand for $\partial F_j/\partial x_j$ and

$$F_{j,j} \equiv \overline{\rho u_j' u_i' u_i'}/2 + \overline{u_i' p'}\delta_{ij} - \overline{f_{ij} u_i'} \tag{B2}$$

$$W \equiv \overline{\rho' u_j'}\,\overline{p}_{,j}/\overline{\rho}^2 \tag{B3}$$

$$\Delta \equiv \overline{p' u_{j,j}'}/\overline{\rho} \tag{B4}$$

$$P \equiv -(\overline{\rho u_i}/\overline{\rho})_{,j}\,\overline{\rho u_j' u_i'}/\overline{\rho} \tag{B5}$$

$$\epsilon \equiv -\overline{f_{ij} u_{i,j}'}/\overline{\rho}. \tag{B6}$$

f_{ij} is the viscous stress tensor

$$f_{ij} = \mu(u_{j,i} + u_{i,j}) - \frac{2}{3}\mu u_{k,k}\delta_{i,j} \tag{B7}$$

where μ is the dynamic viscosity.

The diffusion term $F_{j,j}$ is null in the case of an homogeneous turbulence because all statistical correlation terms are invariant under translation. The pressure work term W which represents the mean velocity-pressure interaction, is equal to zero when the mean pressure is only time dependent. The pressure-dilatation term Δ, which represents the velocity-pressure fluctuations interaction, is null in an incompressible turbulence because the velocity fluctuations are divergence-free ($u_{i,i}' = 0$). Although we have no real information about this divergence, we assume that $u_{i,i}'$ is weak enough when $M_t < 1$ to neglect Δ. Finally the two last terms P and ϵ in the right hand side of Eq. (16) are called, respectively, production (by the mean flow) and dissipation (by viscosity) of the turbulent kinetic energy. Note that the two pressure terms W and Δ vanish in the limit of incompressible flow while all other terms have analogs in the corresponding incompressible equation.

In the case of a spherical compression we have

$$(\overline{\rho u_j}/\overline{\rho})_{,i} = D\delta_{ij}/3 \tag{B8}$$

where D is the compression rate defined by

$$D(t) \equiv (\overline{\rho u_i}/\overline{\rho})_{,i} = -dln\overline{\rho}/dt. \quad \text{(B9)}$$

Thus with all our assumptions, the equation of the turbulent kinetic energy reduces to

$$\frac{dk}{dt} = -\frac{2}{3}Dk - \epsilon. \quad \text{(B10)}$$

A second equation describing the evolution of the dissipation ϵ must be used to close the k-ϵ model. In principle, the exact equation for ϵ can be obtained from the Reynolds equations, but the final equations before modeling, has more than 20 terms in its right side. Thus it is too complicated to be a good starting point for the modeling process, but it is useful as a guide in formulating the ϵ one-equation model (see for instance Reynolds 1980). An appropriate form for low Mach turbulent number ($u_{ii}^{'} \simeq 0$) compressible cases (especially the spherical one) and homogeneous turbulence is (Coleman and Mansour 1991)

$$\frac{d\epsilon}{dt} = -\left[\frac{4}{3}D - \frac{1}{\nu}\frac{d\nu}{dt}\right]\epsilon - C_2\frac{\epsilon^2}{k} \quad \text{(B11)}$$

where ν is the kinematic viscosity. The first term corresponds to the production by action of the mean flow, the second takes into account the variations of ν and the last term expresses the dissipation rate. A usual value for the coefficient C_2, adjusted experimentaly, is 1.92. If the specific heats are assumed constant, the dynamic viscosity μ of the gas is temperature-dependent

$$\mu(T) = \mu(T_0)\left(\frac{T}{T_0}\right)^n \quad \text{(B12)}$$

where $n = \frac{1}{2} + \frac{2}{s-1}$ specifies the interaction force between particles of the gas which is determined by the power law $F_{int} \propto 1/r^s$. The differentiation with respect to time of the relation between dynamic and kinematic viscosities $\mu = \nu\rho$ gives

$$\frac{1}{\mu}\frac{d\mu}{dt} = \frac{1}{\rho}\frac{d\rho}{dt} + \frac{1}{\nu}\frac{d\nu}{dt}. \quad \text{(B13)}$$

We deduce from continuity equation $\frac{d\rho}{dt} = -D\rho$, and from $\frac{d\mu}{dt} = \frac{d\mu}{dT}\frac{dT}{dt} = n\mu\frac{1}{T}\frac{dT}{dt}$, that

$$\frac{1}{\nu}\frac{d\nu}{dt} = D + \frac{n}{T}\frac{dT}{dt} = D - n\Theta \quad \text{(B14)}$$

where $\Theta \equiv -dlnT/dt$. Coleman and Mansour (1991) have assumed an isentropic spherical compression to model the variations of viscosity. Here with Eq. (29), we are in a more general case because we have taken the average temperature of the atmospheric model which is not adiabatic.

Thus the ϵ-equation becomes

$$\frac{d\epsilon}{dt} = -\left[\frac{1}{3}D + n\Theta\right]\epsilon - C_2\frac{\epsilon^2}{k}. \quad \text{(B15)}$$

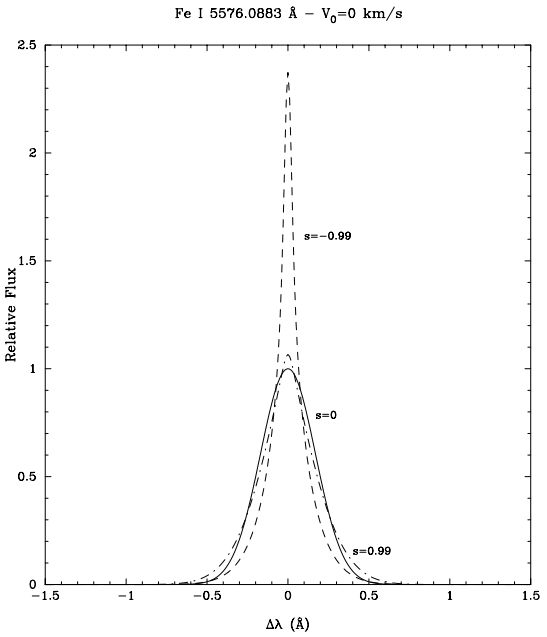

Fig. 5. Metallic line profile (Fe I 5576.0883 Å) for different anisotropy coefficients s for a pulsational velocity V_0 = 0 km/s. The flux is normalized to the s = 0 profile

Appendix B: effect of an anisotropic turbulence on a line profile

For each point of the visible half stellar sphere, the observed velocity (and consequently the Doppler shift) is constituted by the mean radial expansion velocity V_0, the radial and tangential turbulent velocities and the thermal velocity, projected on the line of sight. For the observed velocity, we can construct a probability density law considering that

- the two tangential components of the turbulent velocity $v_{tg}^{'}$ are isotropic and follow a normal law,
- the radial turbulent velocity $v_r^{'}$ also follows a normal law but is independent of that of the tangential components,
- the thermal velocity $v_{th}^{'}$ is isotropic and follows a third independent normal law. Note that the velocity $v_{th}^{'}$ corresponds to the thermal velocity in only one direction.

Consequently, the sum of all these velocity contributions will also be a normal law. For one element of the emitting layer on the half visible sphere, the probability density function of the Doppler shift $\Delta\lambda$ associated with the observed velocity V_0 is

$$P(\Delta\lambda) = \frac{1}{\sqrt{2\pi}\sigma}\exp -\frac{(\Delta\lambda - \mu)^2}{2\sigma^2} \quad \text{(B1)}$$

with

$$\sigma^2 \equiv \left(\frac{\lambda_0}{c}\right)^2 [(v_{th}^{'2} + v_{tg}^{'2})\sin^2\theta + (v_{th}^{'2} + v_r^{'2})\cos^2\theta] \quad \text{(B2)}$$

and

$$\mu \equiv \frac{\lambda_0}{c}\cos\theta\, V_0. \quad \text{(B3)}$$

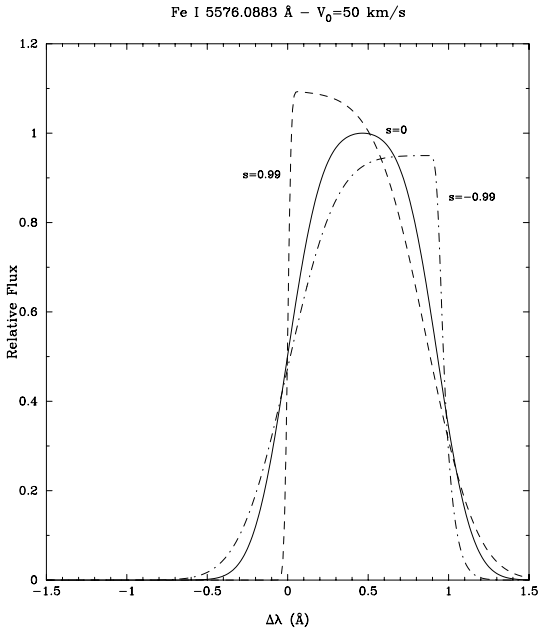

Fig. 6. Same as Fig. 5 but for $V_0 = 50$ km/s

θ is the angle at the center of the star between the point at the stellar surface and the line of sight, λ_0 the laboratory wavelength of the considered absorption line and c the speed of light. We consider that the probability density of $\Delta\lambda$ (Eq. (B1)) is proportional to the specific intensity of radiation I at $\Delta\lambda$. Thus the value of the observed radiative flux F at $\Delta\lambda$ of the center of the absorption line is obtained by integrating the specific intensity I over the stellar half sphere of radius R

$$F(\Delta\lambda) \propto \sqrt{2\pi}R^2 \int_0^{\pi/2} \frac{\sin\theta}{\sqrt{Q^2(1+s\cos 2\theta)}} \times \exp -\frac{(\Delta\lambda - \frac{\lambda_0}{c}V_0\cos\theta)^2}{2Q^2(1+s\cos 2\theta)} d\theta \qquad \text{(B4)}$$

where

$$Q^2 \equiv \frac{\lambda_0^2}{c^2}\frac{2v_{th}'^2 + v_r'^2 + v_{tg}'^2}{2} = \frac{\lambda_0^2}{c^2}q^2 \qquad \text{(B5)}$$

is associated to the bidimensional turbulent energy in the line of sight plane. s is an anisotropy coefficient defined by

$$s \equiv \frac{(v_{th}'^2 + v_r'^2) - (v_{th}'^2 + v_{tg}'^2)}{(v_{th}'^2 + v_r'^2) + (v_{th}'^2 + v_{tg}'^2)} = \frac{v_r'^2 - v_{tg}'^2}{2q^2}. \qquad \text{(B6)}$$

$s = -1$, 0, +1, respectively, for tangential, isotropic and radial turbulence. Nevertheles, if the thermal velocity, which is isotropic, is not negligible, these limits cannot be reached.

The influence of the anisotropy with a constant turbulent kinetic energy Q^2 on an absorption metallic line profile is presented on Fig. 5 without mean dilatational velocity ($V_0 = 0$) and on Fig. 6 with a velocity $V_0 = 50$ km/s. To obtain these profiles, we have used a Q-value such as the temperature of the emitting layer is 5000 K and we have assumed that

$$v_{tg}'^2 + v_r'^2 = 2v_{th}'^2 \qquad \text{(B7)}$$

which seems typical in the atmosphere of δ Cephei. We have forced the limit $s = \pm 0.99$ to illustrate the behavior of the spectral line profile. The departure from the gaussian profile increases with the dilatational velocity V_0. The effect of a turbulent anisotropy on the line broadening is shown on Fig. 2.

References

Achmad L., de Jager C., Nieuwenhuijzen H., 1991, A&A 250, 445
Albrow M.D., Cottrell P.L., 1996, MNRAS 278, 337
Benz W., Mayor M., 1982, A&A 111, 224
Breitfellner M.G., Gillet D., 1993, A&A 277, 524
Butler R.P., 1993, ApJ 415, 323
Coleman G.N., Mansour N.N., 1991, Phys. Fluids A3(9), 2255
Debiève J.F., Gouin H., Gaviglio J., 1982, Indian J. Technol. 20, 90
Debiève J.F., 1983, "Etude d'une interaction turbulence onde de choc", PhD, Aix-Marseille II University
Gillet D., Fokin, A.B., Breitfellner M.G., Mazauric S., Nicolas A., 1998, A&A in press
Fokin A.B., Gillet D., Breitfellner M.G., 1996, A&A 307, 503 (FGB)
Fokin A.B., Gillet D., 1997, A&A 325, 1013
Friedrich R., Bertolotti F., 1997, Appl. Sci. Res. in press
Hanjalic K., Launder, B.E., 1972, J. Fluids Mech. 52, 609
Hannappel, R., Friedrich R., 1995, Appl. Sci. Res. 54, 205
Jaquin L., Cambon, C., Blin, E., 1993, Phys. Fluids A5, 2539 (JCB)
Kovács G., Buchler J.R., 1990, "Confrontation between stellar pulsation and evaluation", eds. Cacciari C. and Clementini G., A.S.P. conference series 11, 226, San Francisco
Kudritzki R.P., 1992, A&A 266, 395
Lamers H.J.G.L.M., Achmad L., 1994, A&A 291, 856
Lee S., Moin P., Lele, S.K., 1992, "Interaction of isotropic turbulence with a shock wave", Report No. TF-52, Department of Mechanical Engineering, Stanford University, Stanford, CA
Mahesh, K., Lele, S.K., Moin, P., 1997, J. Fluid Mech. 334, 353
Mel'nikov O.A., 1950, Trudy, Pulkovo Observ. 64, 47
Mohammadi B., Pironneau O., 1994, "Analysis of the k-ϵ Turbulence Model", Wiley-Masson, Chichester
Reynolds W.C., 1980, "Combustion Modeling in Reciprocating Engines", Eds. Mattavi J.N. and Amann C.A., p41, Plenum Press, New York
Ribner H.S., 1954, NACA Report. No. 1164
Ribner H.S., Tucker M., 1953, NACA Report. No. 113
Rotman D., 1991, Phys. Fluids A3, 1792
Stiff M.J., Gillet D., 1994, "Eighth Cambridge Workshop on Cool Stars, Stellar Systems and the Sun", Ed. Caillault J.P., October 11-14, Athens, GA, USA
Takeda Y., 1995, PASJ 47, 337
van Paradijs J.A., 1971, A&A 11, 299

This article was processed by the author using Springer-Verlag LaTeX A&A style file *L-AA* version 3.